ON-LINE PARAMETER IDENTIFICATION FOR IN-FLIGHT AIRCRAFT MONITORING

G. Hardier*, A. Bucharles*
* Systems Control and Flight Dynamics Department, ONERA The French Aerospace Lab,
Toulouse, France, (e-mail: Georges.Hardier@onera.fr)

Abstract

To improve A/C safety and autonomy, the early detection of unexpected events likely to happen during flight is of primary importance for handling the Flight Control System and providing enhanced cueing of the envelope limits to the pilot. The approach proposed for achieving this on-line monitoring relies on a real time parameter identification technique. Owing to its low computational cost and its robustness regarding measurement noises, an output error method in the frequency domain is developed to estimate the stability and control derivatives of a linearized state-space model. It is the major piece of a monitoring process including also pre and post-processing stages, to prevent from and to filter out inaccurate estimations. Some evaluation results are shown to demonstrate the reliability of the approach. They involve actuator Fault Detection, Isolation and Estimation as well as icing detection, and are compared to a time domain batch algorithm used as a reference method.

1 Introduction

Despite efforts undertaken to improve safety, commercial aircraft accidents continue to occur due to unexpected events like actuator failures or icing. Therefore, a mid-term challenge for Flight Control Systems (FCS) is to recover safely from large aerodynamic changes, structural damage, or system faults. Concerning actuator failures, the usual solution consists in introducing more and more functionally redundant elements in order to achieve the level of reliability necessary for the certification. This solution penalizes the overall system perfor-

mance in terms of weight, power consumption, maintenance needs, etc...

Otherwise, safety requirements for commercial and military airplanes have led to introduce redundant control surfaces into their design, to handle a degradation of the basic airframe configuration (damaged surface). Reconfigurable control [18] can then provide the redistribution of forces and moments along the remaining effectors by using mechanical redundancy. More recently, low-weighted UAV have also been developed for remote sensing, for which autonomy requires the ability to accommodate failures.

The design of a reconfigurable FCS including fault detection results from a trade-off between the speed/accuracy of the response and the robustness/generality of the technique, to minimize both detection delay and rate of false alarms. Usual Fault Detection, Isolation, and Estimation (often referred as FDIE) requires to discover that the plant is not behaving as expected (FD), to determine the real location of the fault (FI), and to find out its exact magnitude (FE). Assuming that a post-fault model is available with an updated set of parameters got by Parameter IDentification (PID), the Fault Accommodation (FA) process is completed by scheduling or redesigning the Fault Tolerant Control (FTC) laws [2,7].

Apart from effector faults and damage, icing is also a major cause of aviation accidents (hundreds of related reports), and is always involved in fatal crashes despite the efforts undertaken to improve the active/passive anti-icing systems [5]. Current IPS (Ice Protection Systems) consist of deicing/anti-icing systems that remove or inhibit ice accretion, as well as stall protection systems that limit the pilot

authority to keep the airplane within a safe flight envelope. As icing sensors are not always available on some commuter A/C, advisory IPS systems are not so safe. Even when sensors are available, they don't evaluate the degradation of the flight dynamics, e.g. due to wing or tail icing. Therefore, for advanced systems like the Ice Management System (IMS) developed during the Smart Icing Systems project, an appropriate PID method proves also to be necessary [12]. Accordingly, different algorithms were studied for icing characterization, which are nothing but a special case of FDI.

There are two categories of methods for FDI, according to whether they make use of a model or not. The latter involve rule-based expert systems or pattern recognition techniques, e.g. using artificial Neural Networks (NN) to learn the diagnosis through repeated training. More conventional FD approaches rely on the use of static or dynamic models, and faults appear as parameter or state changes determined by means of estimation techniques.

Unlike the costly physical redundancy involving several sensors, measured data are compared to analytically obtained values of the variables, by making use of present and past measurements as well as mathematical models describing their relationship (system-wide vs component level monitoring). Thus, the process involves two steps: residual generation from the resulting discrepancies, addressed by deterministic or statistical approaches, and then decision making.

State estimation and observer-based schemes have been widely studied for residual generation [7,15]. Actuator FDIE has also been directly attempted by switching and tuning amongst a set of models. The A/C dynamic response is compared to the output of different models, e.g. a bank of parallel Kalman Filters (KF), each matching a particular fault status of the system [6]. This method can only be applied as long as the expected faults can be hypothesized by a reasonable number of KF. That's why extended KF is often used instead [4], to estimate the unknown fault parameters (e.g. position of a stuck actuator). However, these schemes might perform poorly in real-life problems due to discrepancies between the actual system and the filter model, and to the processing of non-white and biased residuals. More recently, the modeling of any off-nominal behavior by using on-line approximation structures (e.g. NN-based) has also been proposed, but the lack of rigorous analytical proofs of convergence prevents at the moment from certifying such approaches for civil A/C.

Moreover, the complexity of these techniques often exceeds the present limitations of on-board computers, both for code implementation and CPU power. Otherwise, real time PID is often required for indirect adaptation or FTC requiring an updated model. So, when detection precedes accommodation (FDIA) or involves an explicit model (IMS), it makes sense to rely on parameter estimation for the FDI stages too. We only need to assume that the dynamic model can be locally represented by a linear structure with varying parameters to account for changes in the flight condition, failures, or damage.

Using PID for FD makes up a special class of model-based methods, the residuals referring to model parameters instead of system variables [16]. Real time PID faces several problems: external disturbances (e.g. turbulence), measurement noises, and data information content. The technique must estimate changes in the dyna-mics within a short delay despite state and output noises. Time domain methods (TD-PID) usually involve sequential batch or recursive Least-Squares (LS) and require the adjustment of several tuning parameters. Poor information content (e.g. in cruise condition when variables remain constant during extended periods of time) requires strong forms of regularization in the estimation process [15].

On the contrary, frequency domain techniques (FD-PID) have many attractive features. The computation time is greatly reduced by processing only a limited amount of data within the frequency bandwidth of interest. Due to weak excitation signals and large residual errors, a measure of confidence is essential to the accommodation logic and can be easily computed via the standard deviation of the estimation errors. Furthermore, the availability of efficient tools for going from time to frequency domain, like the Fourier Transform (FT), greatly eases the use of FD-PID.

FT Regression (FTR) was thus selected over other algorithms during the Intelligent Flight Control System project [17], and its interest highlighted for a decade [13,14]. More significantly, these tools allow using the Output Error (OE) method (the most powerful to process measurement noises which spoil the A/C states and thus bias the LS estimates), which is not conceivable in the time domain.

De facto, processing short data records and estimating a limited set of parameters result in a well-conditioned optimization problem, and in a fast convergence within one or two iterations most of the time. As shown by this paper, the computational complexity of an OE approach remains quite acceptable against a simpler FTR, Equation Error type (EE). Regarding implementation on aboard computers, there is not much difference between EE and OE algorithms; both of them requires to solve a set of linear equations and can either be used for A/C monitoring.

Regarding the IMMUNE project (cf. the companion paper [3]), the proposed PID method is useful both for event detection (ED) via the variation of aerodynamic parameters, and for event handling since an updated model is often required for indirect adaptation or FTC techniques [10]. In practice, it delivers a near real time estimation of the stability/control derivatives involved in the A/C modelling.

2 Theoretical Development

2.1 From Time to Frequency Domain

The transition from time to frequency domain is classically realized thanks to the standard FT of the signals. As they are only available over a limited period of time [0,T], the finite FT is used instead, which leads to the following relations for a signal $x(t)$, its time derivative, and a constant bias b

$$\begin{cases} x(t) \Leftrightarrow \mathcal{F}_\mathrm{T}[x(t)] = X(\omega,T) = \int_0^T x(t)\, e^{-j\omega t}\, dt \\ \dot{x}(t) \Leftrightarrow \mathcal{F}_\mathrm{T}[\dot{x}(t)] = j\omega\, X(\omega,T) \\ \qquad\qquad + x(T)\, e^{-j\omega T} - x(0) \\ b \;\Leftrightarrow \mathcal{F}_\mathrm{T}[b] = b\,(1 - e^{-j\omega T})\big/ j\omega \end{cases} \quad (1)$$

Practically, from a sampled signal $x(t)$, the finite FT can be approximated by a rectangular nume-rical integration using N values equally spaced over the interval [0,T]

$$X(\omega,T) \approx \Delta t \sum_{n=0}^{N-1} x(n\Delta t)\, e^{-j\omega n\Delta t} = \Delta t\, \widetilde{X}(\omega) \quad (2)$$

The Fast Fourier Transform (FFT) is an efficient tool for computing the Discrete Fourier Transform (DFT) $\widetilde{X}(\omega)$. From N data samples, this algorithm calculates N values of the DFT over the frequency interval [0,$2\pi N/T$], equally spaced too with a step $\Delta\omega = 2\pi/T$. It makes very simple operations possible to evaluate the DFT at time $n\Delta t$ from its previous value at time $(n\text{-}1)\Delta t$ (by denoting $\phi = \omega\Delta t$)

$$\widetilde{X}_n(\omega) = \widetilde{X}_{n-1}(\omega) + [x(n\Delta t)\, e^{-j\phi}]\, e^{-j(n\text{-}1)\phi} \quad (3)$$

For a given frequency ω (and thus a given ϕ), updating the DFT requires only 2 multiplications and 1 addition, i.e. a very low computational effort [9]. When using this recursive FT (RFT), older information can be overweighted regarding to recent ones, which can result in much delay in the monitoring process. To remove the effect of oldest data, it is usual to work on a limited time window $L = l\Delta t$

$$\begin{aligned} \widetilde{X}_n^L(\omega) = \;& \widetilde{X}_{n-1}^L(\omega) \qquad\qquad\qquad (4) \\ & + x(n\Delta t)\, e^{-jn\phi} - x((n-l)\Delta t)\, e^{-j(n-l)\phi} \end{aligned}$$

2.2 From Equation Error to Output Error Minimization

The EE approach is famous (see e.g. [8]). It consists in minimizing the errors between model-predicted and measured forces/moments. When using an OE method, unlike EE, the estimation of state/output biases plus initial conditions is usually advisable to cope with i/o measurement offsets or model structure uncertainties. Consequently, the time domain state equations take the following form

$$\begin{cases} \dot{x}(t) = A(\Theta)x(t) + B(\Theta)u(t) + b_x \qquad (5) \\ y(t) = C(\Theta)x(t) + D(\Theta)u(t) + E(\Theta)\dot{x}(t) + b_y \end{cases}$$

with initial condition $x(0) = x_0$. Matrices A,B,C,D include the stability and control

derivatives Θ to be estimated, assumed to be constant or at least to vary slowly during the flight with respect to the updating process. The state vector x comprises aircraft speeds and angular velocities in body axis, as well as Euler angles. The control vector u collects the control surface deflections, whereas the output measurement vector y includes state compo-nents, air data angles α, β and load factors $Nxyz$.

A matrix E was added to (5.2) to account for a possible dependence of some outputs on state derivatives (which happens e.g. with load factors). Though E could be gathered with C, D terms, this formulation permits to improve the algorithm and the sensitivity computations. By using (1) with ω multiples of the sampling frequency, (5) greatly simplifies to end up in (omitting Θ to alleviate the writing)

$$\begin{cases} j\omega X(\omega) = AX(\omega) + BU(\omega) + b_x T\delta(\omega) + \Delta x \\ Y(\omega) = [C + j\omega E]X(\omega) + DU(\omega) \\ \qquad\qquad + b_y T\delta(\omega) - \Delta x E \end{cases} \quad (6)$$

where $\Delta x = x(0) - x(T)$ denotes the discrepancies between initial and final conditions, $\delta(\omega) = 1$ for $\omega = 0$, and $\delta(\omega) = 0$ else. This Dirac function δ comes from the biases of (1.3) for which $[1 - \exp(-j\omega T)] / j\omega = T$ for $k = 0$ (and 0 else), for $\omega = 2k\pi / T$. Localized effects in the time domain are thus translated into broadband effects in the frequency domain, and vice versa. The initial and final conditions result in a bias which impacts on all frequencies, but the biases which act as broadband inputs in the time domain modify only the zero frequency.

To get the most out of these specificities, it is therefore worthwhile to discard the zero frequency during the identification stage, which avoids estimating the state/output biases. Eq. (6) are thus simplified by removing b_x and b_y terms, and the parameters to be estimated reduce to the aerodynamic derivatives enclosed in Θ and to the vector Δx.

In the time domain, the cost function to be minimized is usually chosen to be a weighted sum of the sampled errors at time t between the measured outputs $z(t)$ and the predicted outputs $y(t, \Theta)$, computed from the current value of the estimated parameters Θ. Summation is taken over the N samples of the time interval $[0, T]$, and the weights correspond to the covariance of the measurement noises (a priori known or jointly estimated in the Maximum Likelihood version). To get the equivalent cost function in the frequency domain, we can turn to Parseval's theorem conveying the principle of energy preservation between the two domains.

Thus, by denoting $\varepsilon(\omega_k, \Theta) = Z(\omega_k) - Y(\omega_k, \Theta)$ and $\dagger$ representing the complex conjugate transpose operator, it can be shown that the resulting cost function is expressed by

$$J(\Theta) = \frac{1}{2} \frac{\Delta f}{\Delta t} \sum_{k=1}^{M} \varepsilon^\dagger(\omega_k, \Theta) \, R^{-1} \varepsilon(\omega_k, \Theta) \quad (7)$$

where the summation is now taken over the M frequencies of interest (equally spaced with a sampling period Δf), issued from the FT of the signals $z(t)$ and $y(t, \Theta)$. In the case of a priori knowledge, a second term should be added in the previous cost expression to penalize the variations of the Θ parameters from their initial values.

The usual way of minimizing a criterion such as the one of (7) consists in using a 2nd order optimization technique (Newton type), and the pros of this algorithm are kept in the frequency domain approach. By differentiating (7), it is easy to prove that the expressions of the gradient and Hessian matrix (usual Gauss-Newton approximation) simply differ from the time domain one by taking the real parts of the summations (see e.g. [9])

$$\begin{cases} \dfrac{\partial J(\Theta)}{\partial \Theta} = -\dfrac{\Delta f}{\Delta t} \mathcal{R}\left[\sum_{k=1}^{M} S^\dagger(\omega_k, \Theta) R^{-1} \varepsilon(\omega_k, \Theta) \right] \\[2mm] \dfrac{\partial^2 J(\Theta)}{\partial \Theta \partial \Theta^T} \approx \dfrac{\Delta f}{\Delta t} \mathcal{R}\left[\sum_{k=1}^{M} S^\dagger(\omega_k, \Theta) R^{-1} S(\omega_k, \Theta) \right] \end{cases}$$

where the sensitivity matrix $\partial Y(\omega_k, \Theta) / \partial \Theta$ is denoted by $S(\omega_k, \Theta)$.

Thanks to the linear modeling, this matrix can be computed analytically without resorting to a finite difference evaluation. The sensiti-vities ($\partial X / \partial \Theta$, $\partial Y / \partial \Theta$ then) can be expressed in terms of the partial derivatives $\partial A / \partial \Theta$, $\partial B / \partial \Theta$, $\partial C / \partial \Theta$, etc... which can be easily derived from the set of linearized equations given in §3.1.

3 Practical Use of the PID for Monitoring

3.1 Nonlinear and Linearized A/C Models

The simplified model of (5), to be used for on-line PID, results from a linearization of the A/C non-linear modeling about the equilibrium conditions (or mean values computed over the time window). The general equations of motion (6 DoF) describing the flight dynamics are not listed herein (see e.g. [1,9]). Assuming a symmetrical aircraft in relation to the vertical plane and no wind, they express in body axes the state derivatives in terms of the aerodynamic forces F_{xyz} and moments M_{xyz}, plus the engine thrusts. The state vector comprises the aircraft airspeed u,v,w at the CG location, and the roll, pitch, yaw rates p,q,r in body axis. The flight mechanics equations are supplemented by the usual kinematic relations expressing the derivatives of Euler attitude angles φ,θ,ψ and altitude h. On the other hand, the measurement equations give access to the flight parameters (α,β), (p,q,r), (φ,θ,ψ), (Nx,Ny,Nz), h and airspeed V in terms of their corresponding measured values at the locations of the IRS and Air Data probes (for α, β). These nonlinear equations serve also as a reference basis for comparisons of the results obtained by the FD-PID and TD-PID (cf. §4). When using the latter method, the aerodynamic parameters will be estimated from the same data during a separate batch identification process, and the results used as reference values for evaluating the linear estimates of the on-line PID method.

At the beginning of each PID stage, from the aerodynamic expressions of forces and moments, a numerical linearization procedure enables to get the initial set Θ_0 of dynamic and control derivatives to be estimated from the current data. The discrepancy between Θ_0 and the estimated vector Θ will also be used by the decision process to detect if some event occurred during the monitored period (cf. §3.2). To be implemented aboard, this nonlinear model must be reliable, computationally efficient, and require a low storage capacity. Accordingly, a modeling of the aerodynamic coefficients by means of local NN is contemplated, linearized onboard to get the reference A,B matrices. It uses a set of Radial Basis Function modules for a white-box representation of the forces and moments (this topic is beyond the scope of this paper; see *www.cert.fr/dcsd/idco/idlon-rn/* for more details). Practically, the longitudinal and lateral/directional cases are treated separately in the identification process. Without going into details, for the lateral case given below as an example, the linearized aerodynamic developments express as (i stands for y, l, n, i.e. for lateral force, roll moment, and yaw moment)

$$Ci = Ci_\beta \frac{v}{V_0} + Ci_p \frac{pL_{ref}}{V_0} + Ci_r \frac{rL_{ref}}{V_0} \qquad (8)$$
$$+ Ci_{\delta_a} \delta_a + Ci_{\delta_r} \delta_r$$

with usual notations for the expansion of the dynamic/control derivatives (δ_a,δ_r aileron and rudder deflections).

According to the FDI process, two different models need to be considered. During the first stage (FD), "ambiguous" actuators (i.e. those for which a detected fault cannot be attributed directly to a single surface) are merged into a unique equivalent actuator. This is the case in longitudinal for right/left elevators (RE/LE), and for right/left Outer/Inner Ailerons δ_{oa}, δ_{ia} in lateral (OA/IA). During the second stage (FI), these actuators are splitted and their real individual deflection restored to enable the improvement of the diagnosis.

The FD and FI models share the same state components $x^T = [v \quad p \quad r \quad \varphi]$ and outputs $z^T = [\beta \quad p \quad r \quad \varphi \quad Ny]$, whereas the input vector is $u^T = [\delta_a \quad \delta_r]$ for the FD stage, but is extended as $u^T = [\delta_{ria} \quad \delta_{lia} \quad \delta_{roa} \quad \delta_{loa} \quad \delta_r]$ for the FI stage. The merged equivalent aileron deflection δ_a is determined by summing the effect of inner and outer (left and right) angles, weighted by their corresponding lever arms.

3.2 Pre-Processing the Data and Post-Processing the Results

It is essential to develop practical means to avoid inaccurate estimation when information is too poor, and to provide confidence in the reliability of the parameters else. This problem is strengthened herein by two facts: ❶ the length of the signals processed will be kept as

short as possible (for reducing the detection delay) ❷ for the FD stage, ordinary control signals resulting from pilot or autopilot orders will be favoured against peculiar excita-tion signals commonly used for PID purposes. In the frequency domain, it is relatively easy to check the information content of the signals. Without any extra calculation, and from Parseval's theorem, the power contained in the different data can be derived from the FT required for the PID method. A set of tests can thus be imple-mented, e.g. from the power $\mathcal{E}(u)/\mathcal{E}(z)$ of the i/o signals and from the percentage $P(z)$ of data samples in the bandwidth with a coherence $\gamma_{\underline{u}z}$ greater than a minimum threshold γ_{min}

$$\mathcal{E}(u) = \int_{\omega_{min}}^{\omega_{max}} \left| U(\omega) \right|^2 d\omega \qquad (resp. \ \mathcal{E}(z) = \cdots)$$

$$P(z) = \frac{card\{\omega \in [\omega_{min}, \omega_{max}] \ / \ \gamma_{\underline{u}z}(\omega) \geq \gamma_{min}\}}{card\{\omega \in [\omega_{min}, \omega_{max}]\}}$$

The coherence function $\gamma_{\underline{u}z}(\omega)$, between the vector u of inputs and the output z, takes its value in [0-1] at frequency ω. It indicates the part of the output spectrum linearly issued from the inputs for each ω. For standard PID, a value greater than $\gamma_{min} = 0.8$ is usually considered to be satisfactory for processing the data with good confidence. This coherence can be easily computed, even in the MISO case, by using the FT already available for the i/o signals

$$\gamma_{uz}(\omega) = \frac{S_{uz}^{\dagger}(\omega) S_{uu}^{-1}(\omega) S_{uz}(\omega)}{S_{zz}(\omega)} \qquad (9)$$

where $S_{uu}(\omega)$ and $S_{zz}(\omega)$ represent the power spectral densities, while $S_{uz}(\omega)$ represent their cross power spectral density. The pre-processing of the (windowed) identification signals stems from a combination of these tests, and from their application to the set of i/o variables. Thresholds were defined for these tests and tuned up from simulation scenarios (§4). They should be roughly tabulated in terms of flight conditions, since useful signals have generally much lower amplitude and power in cruise conditions for instance, than they have after take-off or before landing. It is also noteworthy that some derivatives can be locked to their nominal values if the data content is judged insufficient to provide a reliable esti-mation of these parameters. As a result of this

preprocessing, the PID step can be skipped, waiting for better excitation signals. Apart from avoiding the risk to cope with unreliable parameter estimates (likely to be eliminated by the post-processing), this precaution saves useless CPU time and prevents from encounte-ring numerical problems due to ill-conditioning during the optimization.

On the other hand, the famous Cramer-Rao inequality permits to check the reliability of the estimates. Eq. (8.2) yields an estimated para-meter covariance matrix according to

$$\Lambda = cov(\hat{\Theta}) \approx [\partial^2 J(\Theta) / \partial \Theta \, \partial \Theta^T]_{\Theta = \hat{\Theta}}^{-1} \qquad (10)$$

From Λ, two statistical metrics relative to the estimates can be easily checked: the Cramer-Rao (CR) bound $C_i = \Lambda_{ii}^{1/2}$ for the ith parameter θ_i, and the parameter insensitivity I_i defined by $I_i^2 = 1 / \Lambda_{ii}^{-1}$. I_i represents a conditional standard deviation, all other parameters keeping their optimum values, while C_i represents an uncon-ditional standard deviation, the other parameters taking any value inside the confidence ellipsoid.

However, C_i corresponds only to a lower bound and can't be used directly since its value is usually too optimistic [11]. This problem comes from colored output residuals (modeling errors + not white noises). Thus, the power of noises is not evenly spread over the entire frequency range, but is concentrated within a limited bandwidth corresponding to the rigid body dynamics. In the frequency domain, the processing takes only place within this band, and thus fits much more the noise assumptions. From experience, corrective factors decrease to values from 2 to 3 (instead of 5 to 10 in the time domain).

In the following, we will choose $C_i^* = 3C_i$. Usual guidelines for reliable estimates suggest also to consider upper limits for the uncer-tainties, i.e. $C_i^* / \hat{\theta}_i \leq \tau_C$ and $I_i / \hat{\theta}_i \leq \tau_I$, with advocated values $\tau_C = 20\%$ and $\tau_I = 10\%$ [1]. Applying this material to the process of moni-toring results in the following steps (by denoting θ_{i0} the initial value of the parameter θ_i):

▪ if $/ \hat{\theta}_i - \theta_{i0} / \leq C_i^*$ or $C_i^* / \hat{\theta}_i \leq \tau_C$ or $I_i / \hat{\theta}_i \leq \tau_I$ then the parameter variation is assumed non significant; else, the PID estimate is validated for a possible event detection

▪ compute a confidence index in the result

$ci = 1 - \min(1, C_i^* / |\hat{\theta}_i - \theta_{i0}|)$, taking its values between 0 and 1 (Fig. 1)

▪ use the relative variation of the coefficient $|\hat{\theta}_i - \theta_{i0}| / |\theta_{i0}|$ to decide how significant the failure can be.

   Thus, this post-processing stage permits to get highest confidence in the estimation, and to filter out any inaccurate result which could increase the rate of false alarms.
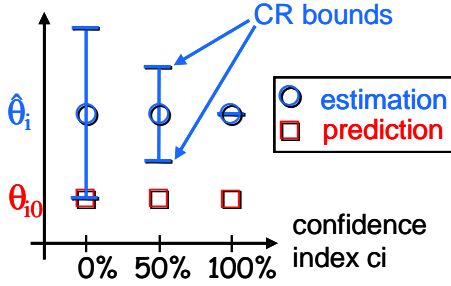

Fig. 1. Confidence index from CR bounds.

3.3 Main Stages of the Event Detection and Isolation Process

The comprehensive scheme of Fig. 2 lets appear 3 instantiations of the FD-PID devoted to the 3 successive steps of the monitoring process (ED, FI if necessary, and possibly FE). Practically, if a partially resolved fault is revealed at the end of the preliminary ED stage, after a request to the supervisor asking for an agreement, a set of superimposed excitation signals is added to the pilot or autopilot orders to ease the determination of the individual surface involved in the fault (FI among a set of "ambiguous" effectors). The choice of these signals results from a balance between unsuitable motions in terms of crew and passenger comfort and the need to get reliable parameter estimates. Herein, it is solved by using sine wave excitations, which are simultaneously applied to the "ambiguous" control surfaces at selected frequencies different from each other. This means permits to avoid correlation problems between the inputs, while keeping very low levels of signals [17]. To avoid unsuitable motions as much as possible, weak amplitudes (e.g. 1° for elevators and 5° for ailerons) and high frequencies (from 0.5 to 1Hz) were selected for these sine functions.

   When a (successful) FD or FI emphasizes some specific faults (jam, ended runaway, stuck actuator), they are expressed at this stage by a

null residual efficiency. The reason is that the frequency method can't distinguish between a 100% loss of efficiency (LoE) and a locked surface when the zero frequency is removed from the processing. However, when the faulty actuator has been isolated, it is possible to interpret a non zero time domain bias - like b_x in (5) - as a constant surface deflection, by using the nominal value of its control derivative coefficient. Conversely, the estimation of a null b_x would confirm the assumption of a total LoE for the actuator. The purpose of the FE is thus to proceed to the estimation of the b_x components from the same isolation data, in order to clear up this ambivalence and to perfect a complete description of the fault. Consequently, the use of the FD-PID for isolation or estimation is not systematic, and is reserved to "ambiguous" effectors or cases (special types of faults).
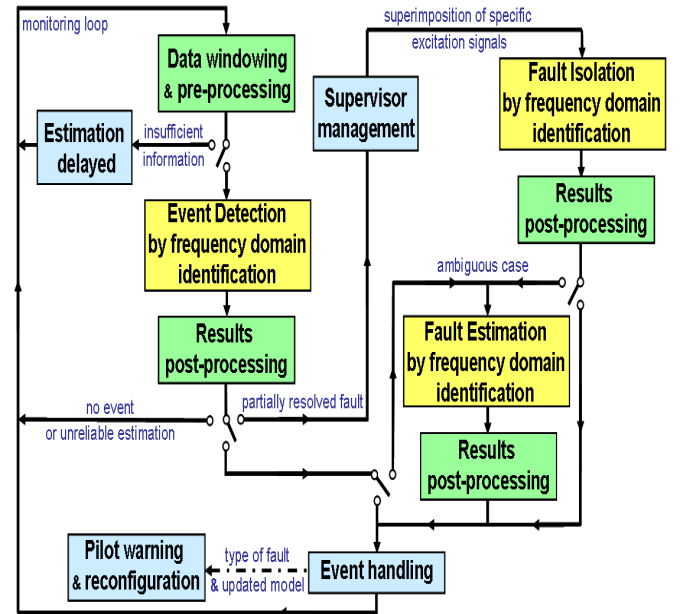

Fig. 2. Overall scheme of the FDIE process.

   The monitoring loop involves also two important parameters. ❶ The width of the receding time window balances the amount of information conveyed by the data (impacting on the accuracy of the estimates) against the sensitivity to ED. A too large window would produce transient values between nominal/faulty parameters and erroneous linear assumptions in case of varying flight conditions. ❷ The updating rate results from another tradeoff between the detection delay and the CPU power of onboard computers. The periodicity of the

updates should also be less than the size of the receding window but should keep the same order of magnitude. A careful evaluation through as set of simulations led to choose a window of length 20s and an updating rate of 10s, except in turbulent conditions where the width of the window was doubled to improve the signal-to-noise ratio. With these choices, the procedure runs 8 times faster than real time on a standard PC. For longitudinal plus lateral monitoring at the same rate, this yields a ratio of 4.

4 Simulation Results

4.1 Icing Detection via On-line PID of the Longitudinal Model

A Matlab/Simulink© desktop simulator was developed during the IMMUNE project. The A/C model is representative of the behavior of a generic long range commercial aircraft (cf. overview [3]). It permits to simulate iced flight conditions by using an additive icing model computing the aerodynamic coefficients in a wide range of situations: no icing, icing with deicing system on/off, level of ice more or less severe. The icing detection is restricted to the longitudinal parameters for which the most significant variations of magnitude are expected. Only the main coefficients of the model are freed to ease the PID from poor excitation signals. The damping derivatives are thus frozen to their reference values to prevent from correlation issues. Thus, the set of coefficients is restricted to $Cz_\alpha, Cz_{\delta e}, Cm_\alpha, Cm_{\delta e}$ and possibly Cz_0, Cm_0 when the zero frequency is not excluded (TD-PID).

At the beginning of the simulated tests, the airplane (in clean configuration) is trimmed at the following equilibrium condition: altitude 700ft, speed 200kts, weight 155t, balance 30%. The Test#1 corresponds to a pilot-input pitch doublet, and the Test#2 to a heading change maneuver from stick orders with autopilot disengaged. As previousuly mentioned, for each evaluation scenario, an OE batch TD-PID is run in parallel to the FD-PID in order to ease the analysis of on-line results and to serve as a comparison basis. By processing the same noisy signals in batch mode, this alternative PID is assumed to produce the best parameter estimates which can be derived from the available data. It deals with the same parameters plus the bias components. However, it relies on the nonlinear A/C modeling instead of linearized versions, and the estimated parameters correspond to linear increments added to the nonlinear aerodynamic coefficients. The results are given in Table 1, estimates being declared non significant (ns) for $Cz_{\delta e}, Cm_{\delta e}$ by the post-processing stage, regarding the corrected CR bounds (the same with TD-PID).

Results are satisfactory for Test#1, similar estimates being provided by both methods, in agreement with the reference values. Test#2 reveals a discrepancy, the results of the FD-PID departing noticeably from the reference, especially for the lift coefficient. This is explained by the type of this test, a lateral-directional maneuver with a low excitation level of the longitudinal actuators. However, even in this (poor) case, the coefficient variations and confidence index are significant enough to output a warning message to the decision module.

Table 1. Iced aircraft: coefficients changes (%)

		Cz_α	Cz_0	Cm_α	Cm_0
reference value		-20.4	+45.5	+19.1	-28.8
Test #1	FD-PID	-16.0	-	+17.9	-
	TD-PID	-18.6	+38.9	+18.1	-26.9
Test #2	FD-PID	-48.0	-	+27.1	-
	TD-PID	-25.8	+63.1	+20.2	-33.3

4.2 Actuator FDIE via On-line PID of the Lateral and Longitudinal Models

To simplify, the successive FD/FI/FE stages were gathered into a single flight, corresponding to an approach: airplane in high lift configuration initially trimmed at 700ft, 150kts (weight 155t, balance 30%). Maneuvers involve small heading adjustments with AP engaged. Only the lateral results are presented for the FD stage. The first 2 minutes of the test are devoted to FD, while the next 20s are kept for FI/FE, assuming that an external decision process (supervisor) has ordered the addition of isolation signals to the actuator deflections from 125 to 145s (see Fig. 3 for a display of the main lateral states and

control orders). For the same reasons as in §4.1, the estimation process is restricted to $Cy_\beta, Cl_\beta, Cl_{\delta_{ia}}, Cl_{\delta_{oa}}, Cn_\beta, Cn_{\delta_r}$ and optionally Cy_0, Cl_0, Cn_0. The sequence of faults/damage is scheduled as follows: at t=30 the right IA is subject to a 50% LoE, just as the right elevator at t=60, finally the left OA is jammed at 5° of deflection at t=90 and simultaneously the rudder is subject to a 40% LoE. At first, the working of the on-line FD process is thus simulated from 0 to 120s (cf. Table 2). Fig. 4 represents the estimates norma-

lized against the expected values for the 11 runs of the FD stage from 0 to 100s (11 windows). Error bars represent CR uncertainties, squares (□) predicted values, white circles (○) valid results, and black ones (●) invalid estimates rejected by the PID process. These results show that the pre and post-processing stages are very useful to filter out unsuited time windows, when the data content doesn't allow for a reliable estimation; e.g. all or part of the coefficients can be frozen after the pre-processing (see it 2).
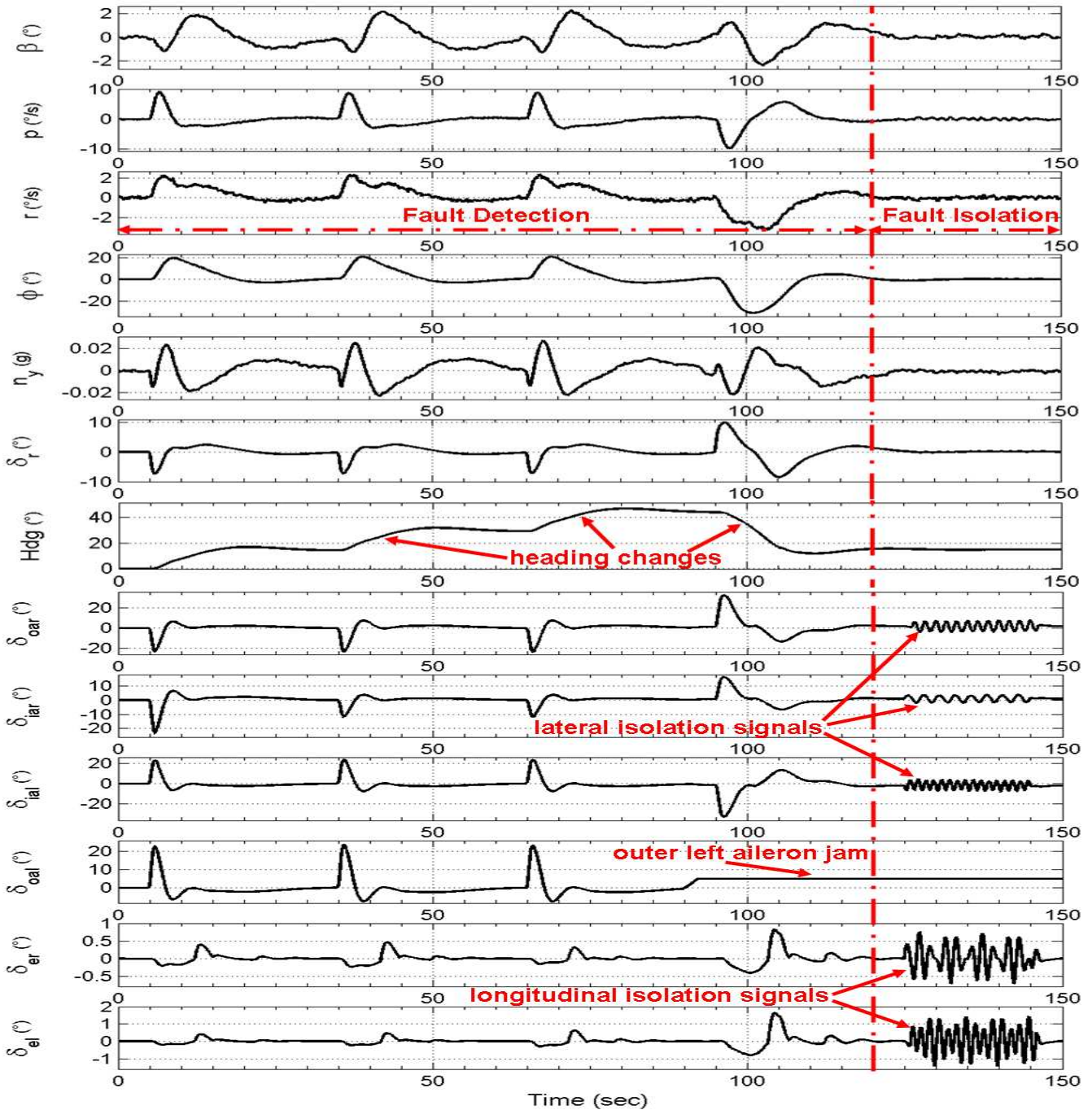

Fig. 3. Lateral/directional states and splitted control surfaces during FD/FI stages.

Table 2. Estimated/expected reductions (%)
of control derivatives during the FD stage

it.	$Cl_{\delta a}$	$Cn_{\delta r}$	it.	$Cl_{\delta a}$	$Cn_{\delta r}$
1	0/0	0/0	7	10.6/11.4	0/0
2	-/0	-/0	8	ns /11.4	0/0
3	11.3/11.4	0/0	9	29.8/38.6	42.8/40
4	10.5/11.4	0/0	10	37.2/38.6	33.8/40
5	ns /11.4	0/0	11	38.2/38.6	25.4/40
6	11.0/11.4	0/0			
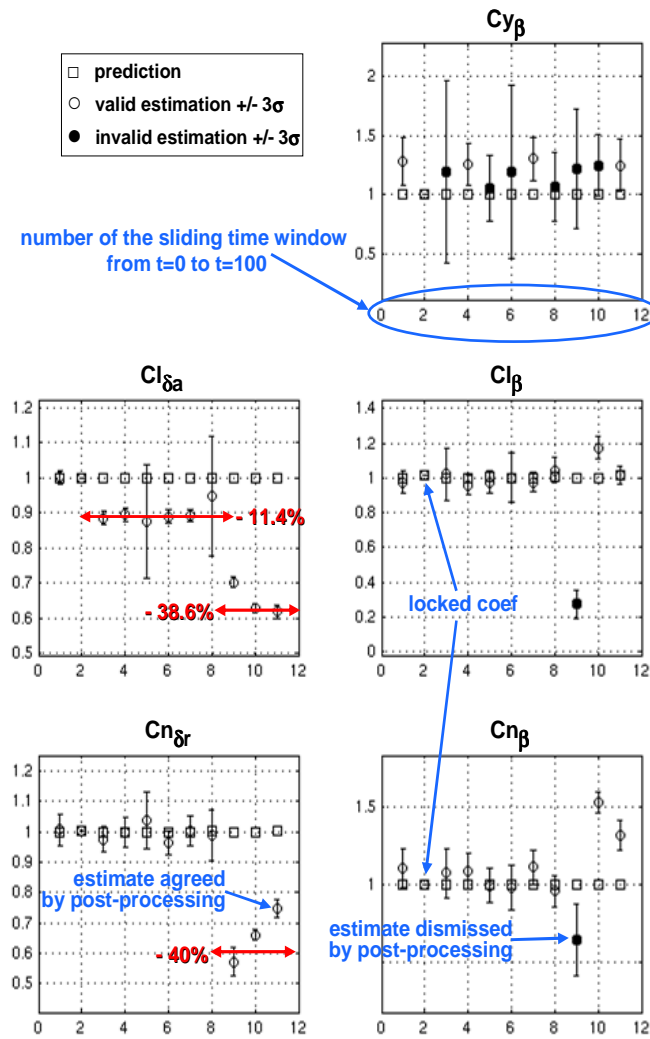
Fig. 4. Lateral/directional FD during approach.

The reference targets, which should ideally be estimated owing to the faults, are displayed as horizontal arrows labeled with the percentages of expected decreases. It's noteworthy that the expected 11.4% and 38.6% reductions for $Cl_{\delta a}$ are not round figures due to the difference of efficiency between IA and OA, lumped into the equivalent aileron deflection δ_a. As mentioned in §3.3, the left OA jam at 90s

amounts at this FD stage to a 100% LoE for this surface (it 10-11). Some apparent discrepancies between expected and estimated values can also be explained by the short length of the time interval, leading to transient values when the fault occurs within the window (e.g. $Cl_{\delta a}$ at it 9). At last, a balance really do exist concerning the input powers, since fast variations of states (like α or β) can compromise the validity of the linearity assumptions. This is the case around 100s, which explains the poorer accuracy of Cn_β and $Cn_{\delta r}$ at it 10-11. Despite these imperfections, the quality of the estimates, and their consistency over the successive runs, appear to meet the requirements of this FD stage.

The faulty situations detected for ailerons from it 3 remain "ambiguous" cases since they can't be assigned to a single control surface at this stage. At the end of the FI stage processing the window from 125 to 145s, all the faults were properly isolated (Tables 3-4 and Fig. 5), and the left OA (LOA) was rightly credited with a 100% LoE (see $Cl_{\delta loa}$). In Tables 3-4, only the estimates denoted with [*] were validated by the post-processing. Others are reasonably accurate but uncertainty is too high. Longitudinal FI is the most difficult case due to a very low signal-to-noise ratio (only 1° for sine signals). A partial indetermination between RE and LE remains (check by summing Table 4 corresponding variations). Besides, TD-PID results are even worse thanks to the noise filtering outside the selected bandwidth which benefits to FD-PID.

Table 3. Estimated variations (%)
of lateral control derivatives after FI stage

	$Cl_{\delta ria}$	$Cl_{\delta ia}$	$Cl_{\delta roa}$	$Cl_{\delta loa}$	$Cn_{\delta r}$
expected value	-50	0	0	-100	-40
FD-PID	-49.5[*]	-0.2	+1.8	-100[*]	-37.3[*]
TD-PID	-50[*]	-1.4	+0.2	-100[*]	-38.6[*]

However, it is not possible at this stage to conclude about the LOA total LoE: complete breakdown, float failure, lock-in-place surface ?. As quoted in §3.3, the FE step serves to refine the diagnosis by simply extending FD-PID to the zero frequency. After having the efficiencies of the faulty actuators adjusted by using the results of the FI stage, the only remaining

parameters to be estimated are Cy_0, Cl_0, Cn_0. As expected, only the Cl_0 estimate appears reliable and leads to a bias equal to 0.016. By dividing this value by the OA efficiency, an equivalent deflection of 4.7° is got, close to the ideal value of 5°. The same results are got with the TD-PID.

Table 4. Estimated variations (%)
of longitudinal control derivatives after FI stage

	$Cz_{\delta re}$	$Cm_{\delta re}$	$Cz_{\delta e}$	$Cm_{\delta e}$
expected value	-50	-50	0	0
FD-PID	-61.8	-40.7[*]	+10.6	-11.4
TD-PID	-66.4	-37.3[*]	+9.6	-8.1
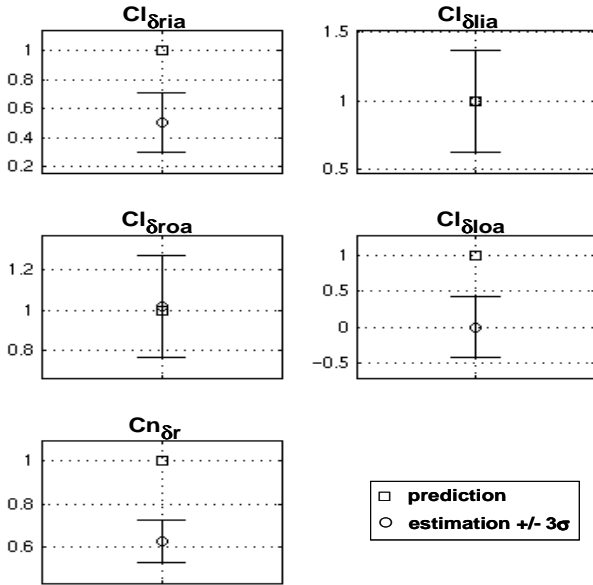
Fig. 5. FI results for lateral control derivatives.

5 Conclusions

To fulfill the requirements of an onboard implementation, a FD-PID algorithm was developed based on an OE formulation, for estimating in real time the parameters of a linear(ized) A/C modeling. The contemplated applications involve the early detection of unexpected events (e.g. icing), the global process of actuator fault diagnosis, and the updating of models to be used by FTC methods. They extend from military and civil A/C to the UAV domain. The methodology includes pre and post-processing stages in addition to the central estimation part, as well as the superimposition of predefined excitation signals for the isolation of some ambiguous effector faults if necessary. The approach, evaluated through a set of realistic flight scenarios involving on-line monitoring of the control surfaces, showed that the method was able to provide satisfactory results (regarding the parameter estimates but also their accuracy) despite of high measurement noises, moderate turbulence and low information content in the data. To ensure a realistic evaluation of the performances, only usual (poor) flight maneuvers were exploited with the AP engaged or disengaged. The computational feasibility of an aboard implementation was also demonstrated. Owing to its characteristics, the FD-PID algorithm requires a few iterations to converge, and the memory requirements are limited thanks to the moving data windowing.

As far as actuator failures are concerned, LoE, jams, runaways and float failures can be detected and recognized through the three steps of the FDIE procedure. For longitudinal failures, the tests have shown that usual maneuvers (like altitude changes) are not always sufficient to monitor the stabilizer and elevators in certain flight conditions (e.g. cruise). Moreover, they stressed the trade-off between the level of excitation, likely to produce fast and large variations of the angle of attack (AoA), and the underlying assumption of linearity peculiar to the frequency domain method. As a result, the most suitable flight conditions for longitudinal FD correspond to low/medium AoA, in clean or high lift configurations. This holds also for lateral FD. On the other hand, usual maneuvers (like small heading changes) are generally adequate for the monitoring process of lateral failures, which proves to be more robust and less sensitive to turbulence than the longitudinal one. Considering icing detection, the model used herein has a very weak effect on the aerodynamic coefficients at low AoA, since it changes mainly the nonlinear behavior regarding the stall AoA. Consequently, significant variations of parameters appear only when non linearities begin to arise, and the flight conditions favorable to an early detection of the icing are therefore medium/high AoA, in clean lift configuration.

Future works should address the usual weak points of most on-line PID methods, i.e.

their robustness to unmodeled disturbances (turbulence) and to low data information content during extended periods of time. For the first point, it should be checked to what extent a supplementary EE approach (less sensitive to state noises) could provide better results in case of strong turbulence. From the OE formulation, its implementation would be straightforward and its use could be reserved to high state-to-measurement noise ratios. The problem of poor data content is somewhat more difficult. Currently, it falls to the pre-processing stage to filter out these periods to prevent from useless PID and possibly inaccurate estimations. This stage could be refined by calling for adaptive thresholds in the decision making, e.g. depending on the flight condition and/or the type of maneuver. More generally, to maintain detection capabilities during long intervals of steady flight, the question of adding artificial excitations to the control orders should be considered, as it was done for the FI stage.

Finally, with the prospect of a global FDD/FTC system, the combined monitoring + handling performances should be evaluated. Depending on the type of FTC method (self-adaptation or reconfiguration), the accommodation process will make use of all or part of the PID results (isolated faults, estimated stuck deflections, adjusted model, coefficients used for gain scheduling,...).

References

[1] Carnduff SD and Cooke AK. Formulation and system identification of the equations of motion for a dynamic wind tunnel facility, Cranfield University, Rept No 0801, 2008.

[2] Chandler PR, Buffington J and Patcher M. Integration of on-line system identification and optimization-based control allocation, *AIAA GNC*, paper 4487, Boston, USA, 1998.

[3] Döll C, Hardier G, Varga A and Kappenberger C. IMMUNE project: an overview, *18th IFAC ACA symposium*, Nara, Japan, 2010.

[4] Ducard G and Geering, HP. A reconfigurable FCS based on the EMMAE method, *ACC*, Minneapolis, USA, pp. 5499-5504, 2006.

[5] Gingras DR, Barnhart B et al. Envelope protection for in-flight ice contamination, *47th AIAA ASM*, paper 1458, Orlando, USA, 2009.

[6] Hanlon PD and Maybeck PS. Multiple-model adaptive estimation using a residual correlation Kalman filter bank, *IEEE trans. on aerospace and electronic systems*, 36 (2), pp. 393-406, 2000.

[7] Hwang I, Kim S, Kim Y and Seah CE. A survey of fault detection, isolation, and reconfiguration methods, *IEEE trans. on control systems technology*, 18, 18 pages, 2010.

[8] Jategaonkar RV. *Flight vehicle system identification: a time domain methodology*, AIAA Ed. Series, Reston, pp. 177-218, 2006.

[9] Klein V and Morelli E. *Aircraft system identification : theory and practice*, AIAA Ed. Series, Reston, pp. 225-287, 2006.

[10] Lafourcade L, Cumer C and Döll C. Control reallocation after surface failures using Model Predictive Control, *18th IFAC ACA symposium*, Nara, Japan, 2010.

[11] Maine RE and Iliff KW. Use of Cramer-Rao bounds on flight data with colored residuals, J^{al} *of guidance, control, & dynamics*, 4 (2), pp. 207-213, 1981.

[12] Melody JW, Basar T et al. Parameter identification for inflight detection and characterization of aircraft icing, *Control engineering practice*, 8, pp. 985-1001, 2000.

[13] Morelli E. Real-time parameter estimation in the frequency domain, J^{al} *of guidance, control, & dynamics*, 23 (5), pp. 812-818, 2000.

[14] Morelli E. Practical aspects of the equation-error method for aircraft parameter estimation, *AIAA AFM*, paper 6144, Keystone, USA, 2006.

[15] Pachter M, Smith L and Chandler PR. Regularization techniques for real-time identification of aircraft parameters, *AIAA GNC*, New Orleans, USA, pp. 1466-1480, 1997.

[16] Patton RJ, Simani S and Fantuzzi C. *Model-based fault diagnosis in dynamic systems using identification techniques*, Advances in Industrial Control, Springer, London, pp. 1-156, 2003.

[17] Smith MS, Moes TR and Morelli E. Real-time stability and control derivative extraction from F-15 flight data, NASA TM-212027, 2003.

[18] Zhang Y and Jiang J. Bibliographical Review on Reconfigurable Fault-Tolerant Control Systems, *Annual Reviews in Control*, 32 (2), pp. 229-252, 2008.